JOURNAL OF COMPUTATIONAL PHYSICS: 6, 17–28 (1970)

Difference Method for Multiple Reflection of Elastic Stress Waves*

S. S. CHIU

Sandia Laboratories, Sandia Corporation, Analytic Mechanics Division, Livermore, California 94550

Received August 14, 1969

This paper presents an original method, using finite-difference approximations, for solving problems of stress-wave propagation in an elastic bar with discontinuities. The method, which is also applicable to similar problems in optical, acoustical, and electrical transmission lines, is simple and amenable to hand computation. With a computer, cases involving hundreds of discontinuities, as well as multiple-reflection problems with randomly related transit-time intervals, can be handled with ease. The validity and versatility of the method are demonstrated by solving two illustrative examples; results are shown to be in good agreement with corresponding analytical and experimental results.

INTRODUCTION

The transmission and reflection of stress waves in an elastic bar with discontinuities have been extensively studied [1–7]. Numerous methods, ranging from simple graphical to sophisticated computer approaches, are available for describing these phenomena. Most of these are based on the ray-tracing method of optics; every discontinuity sets up a series of reflected and transmitted amplitudes, which are followed individually through the system. This paper presents a new approach using finite differences.

STATEMENT OF PROBLEM

It is desired to solve the initial-and-boundary-value problem related to an elastic bar composed of axially symmetric sections of different material properties and cross-sectional areas, as shown in Fig. 1.

The mathematical statement of the problem is as follows. The governing equation is

$$\partial^2\sigma(x, t)/\partial t^2 = c^2(\partial^2\sigma(x, t)/\partial x^2) \tag{1}$$

* This work was supported in part by the U.S. Atomic Energy Commission and by the U.S. Army Research Office (Durham).

581/6/1-2

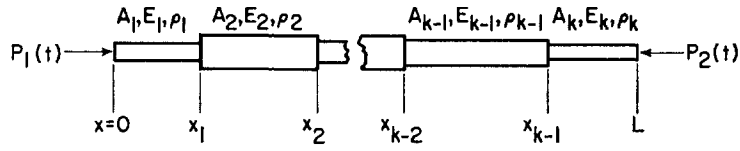

FIG. 1. Bar with discontinuities.

where $0 < x < x_1$, $x_1 < x < x_2, \ldots, x_{k-1} < x < L$ and $t > 0$. The initial conditions are

$$\sigma(x, 0) = f(x) \tag{2}$$

$$\partial\sigma(x, 0)/\partial t = g(x) \tag{3}$$

where $0 < x < x_1$, $x_1 < x < x_2, \ldots, x_{k-1} < x < L$. The boundary conditions are

(1) the prescribed end conditions:

$$\sigma(0, t) = P_1(t) \quad \text{for} \quad t > 0 \tag{4}$$

$$\sigma(L, t) = P_2(t) \tag{5}$$

(2) the conditions for continuous displacements and forces at the interfaces,

$$u(x_{i-0}, t) = u(x_{i+0}, t) \tag{6}$$

$$A_i\sigma(x_{i-0}, t) = A_{i+1}\sigma(x_{i+0}, t) \tag{7}$$

where $i = 1, 2, \ldots, k-1$ and $t \geqslant 0$.

THEORY

The finite-difference method is a powerful tool in solving initial-and-boundary-value problems. The key to a successful solution lies in satisfying the criteria of stability and convergence [8]. The difference solution to the classical wave equation, a second-order, hyperbolic, partial differential equation, is well known. There has been no previous difference solution, however, to the title problem, which involves a mixed boundary condition related to the interface of a discontinuous bar. Though the problem is here limited to stress waves in solids, the method applies equally well in other fields where similar governing equations and boundary conditions prevail.

In the application presented here, two main explicit difference schemes are used, one for the interior points of each section of the bar and one for the interface

boundaries between sections. At the bar ends, where stresses are prescribed, no computations are required.

In this section, the difference scheme for the interior points is reviewed briefly, and the scheme for the interface boundaries is derived in detail.

Interior Points

The following relations are needed for deriving the wave equation (1):

(1) Hooke's law

$$\sigma(x, t) = E\,\epsilon(x, t), \tag{8}$$

(2) definition of strain

$$\epsilon(x, t) = \frac{\partial u(x, t)}{\partial x}, \tag{9}$$

(3) equation of motion

$$\rho \frac{\partial^2 u(x, t)}{\partial t^2} = \frac{\partial \sigma(x, t)}{\partial x}. \tag{10}$$

Using the notation

$$\sigma_{m,n} \equiv \sigma(m\,\Delta x, n\,\Delta t) \tag{11}$$

and central differences, (1) can be approximated as follows:

$$\frac{\sigma_{m,n+1} - 2\sigma_{m,n} + \sigma_{m,n-1}}{\Delta t^2} = c^2 \frac{\sigma_{m+1,n} - 2\sigma_{m,n} + \sigma_{m-1,n}}{\Delta x^2}. \tag{12}$$

The criteria for stability and convergence require [8] that

$$c\,\Delta t/\Delta x \leqslant 1. \tag{13}$$

For the sake of simplicity, the value

$$c\,\Delta t/\Delta x = 1 \tag{14}$$

is preferred and used throughout this paper. Combining (12) and (14), therefore, leads to the expression

$$\sigma_{m,n+1} = \sigma_{m-1,n} + \sigma_{m+1,n} - \sigma_{m,n-1} \qquad \text{for} \quad n \geqslant 1. \tag{15}$$

This is the required difference scheme for the interior points.

Equation (15) is an explicit formula for the calculation of a single value on a new time step, $n + 1$, in terms of known values on the two previous steps, n and

$n - 1$. To start the *marching* process, the first two rows, $n = 0$ and $n = 1$, must be obtained from the prescribed initial values. Equation (2) gives

$$\sigma_{m,0} = f(m\,\Delta x). \tag{16}$$

Expressing (3) by central differences yields

$$\sigma_{m,1} = \sigma_{m,-1} + 2\Delta t\, g(m\,\Delta x). \tag{17}$$

Setting $n = 0$ in (15) yields

$$\sigma_{m,1} = \sigma_{m-1,0} + \sigma_{m+1,0} - \sigma_{m,-1}\,. \tag{18}$$

To eliminate the fictitious term $\sigma_{m,-1}$, one combines (17) and (18) to obtain

$$\sigma_{m,1} = \tfrac{1}{2}(\sigma_{m-1,0} + \sigma_{m+1,0}) + \Delta t\, g(m\,\Delta x). \tag{19}$$

Equations (15), (16), and (19) provide the necessary means for solving initial-value problems for interior points.

Interface Boundary

Consider an infinitely long bar with a single discontinuity, as shown in Fig. 2. The cross-sectional area and material properties are different on either side of the discontinuity. It is convenient to choose the coordinate system so that $x = 0$ is at the discontinuity.

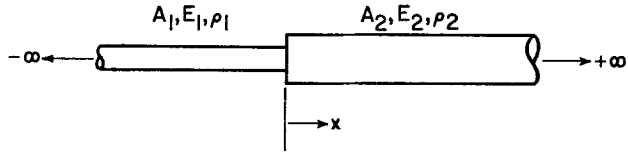

FIG. 2. Interface of a discontinuous bar.

Equation (6) gives

$$u(0^-, t) = u(0^+, t). \tag{20}$$

Hence

$$\frac{\partial^2 u(0^-, t)}{\partial t^2} = \frac{\partial^2 u(0^+, t)}{\partial t^2}\,. \tag{21}$$

Equation (10) gives

$$\rho_1 \frac{\partial^2 u(0^-, t)}{\partial t^2} = \frac{\partial \sigma(0^-, t)}{\partial x} \tag{22}$$

and

$$\rho_2 \frac{\partial^2 u(0^+, t)}{\partial t^2} = \frac{\partial \sigma(0^+, t)}{\partial x}. \tag{23}$$

Equations (21), (22), and (23) are then combined as follows:

$$\frac{1}{\rho_1} \frac{\partial \sigma(0^-, t)}{\partial x} = \frac{1}{\rho^2} \frac{\partial \sigma(0^+, t)}{\partial x}. \tag{24}$$

Equation (1) gives

$$\frac{\partial^2 \sigma(0^-, t)}{\partial t^2} = {c_1}^2 \frac{\partial^2 \sigma(0^-, t)}{\partial x^2} \tag{25}$$

and

$$\frac{\partial^2 \sigma(0^+, t)}{\partial t^2} = {c_2}^2 \frac{\partial^2 \sigma(0^+, t)}{\partial x^2}. \tag{26}$$

Equation (7) gives

$$A_1 \sigma(0^-, t) = A_2 \sigma(0^+, t). \tag{27}$$

Hence

$$A_1 \frac{\partial^2 \sigma(0^-, t)}{\partial t^2} = A_2 \frac{\partial^2 \sigma(0^+, t)}{\partial t^2}. \tag{28}$$

Equations (25), (26), and (28) are then combined as follows:

$$A_1 {c_1}^2 \frac{\partial^2 \sigma(0^-, t)}{\partial x^2} = A_2 {c_2}^2 \frac{\partial^2 \sigma(0^+, t)}{\partial x^2}. \tag{29}$$

Equations (24), (27), and (29) provide the relations of the stresses and their spatial derivatives at the discontinuity.

For the difference solution, the spatial grids are chosen as shown in Fig. 3. The grid sizes depend on the wave velocities of the materials and the time increment, Δt, which is chosen by considering pulse shape and bar length. Equation (14) gives

$$\Delta x_1 = c_1 \Delta t \tag{30}$$

and

$$\Delta x_2 = c_2 \Delta t. \tag{31}$$

Equations (30) and (31) yield

$$\Delta x_1 / \Delta x_2 = c_1 / c_2. \tag{32}$$

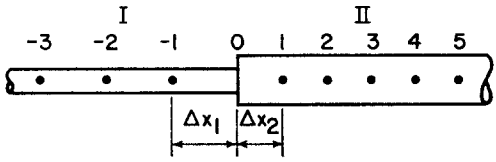

FIG. 3. Difference grids.

Using Taylor's expansion for both sides of the interface and neglecting higher than second-order terms yields

$$\sigma_{-1,n} = \sigma_{0^-,n} - \Delta x_1 \frac{\partial \sigma}{\partial x}\bigg|_{0^-,n} + \frac{1}{2}\Delta x_1^2 \frac{\partial^2 \sigma}{\partial x^2}\bigg|_{0^-,n} \tag{33}$$

and

$$\sigma_{+1,n} = \sigma_{0^+,n} + \Delta x_2 \frac{\partial \sigma}{\partial x}\bigg|_{0^+,n} + \frac{1}{2}\Delta x_2^2 \frac{\partial^2 \sigma}{\partial x^2}\bigg|_{0^+,n}. \tag{34}$$

Equation (34) can be expressed in terms of the left side values $(0^-, n)$ by incorporating (24), (27), and (29):

$$\sigma_{+1,n} = \frac{A_1}{A_2}\sigma_{0^-,n} + \Delta x_2 \frac{\rho_2}{\rho_1}\frac{\partial \sigma}{\partial x}\bigg|_{0^-,n} + \frac{1}{2}\Delta x_2^2 \frac{A_1}{A_2}\left(\frac{c_1}{c_2}\right)^2 \frac{\partial^2 \sigma}{\partial x^2}\bigg|_{0^-,n}. \tag{35}$$

The first derivative in (35) may be eliminated by solving (33) and (35):

$$\frac{1}{2}\Delta x_1^2\left[\frac{\Delta x_2}{\Delta x_1}\frac{\rho_2}{\rho_1} + \frac{A_1}{A_2}\left(\frac{\Delta x_2}{\Delta x_1}\right)^2\left(\frac{c_1}{c_2}\right)^2\right]\frac{\partial^2 \sigma}{\partial x^2}\bigg|_{0^-,n}$$
$$= \sigma_{+1,n} - \frac{A_1}{A_2}\sigma_{0^-,n} - \frac{\Delta x_2}{\Delta x_1}\frac{\rho_2}{\rho_1}[\sigma_{0^-,n} - \sigma_{-1,n}]. \tag{36}$$

Equations (25), (32), and (36) are then combined as follows:

$$\frac{1}{2}\Delta x_1^2\left[\frac{c_2\rho_2}{c_1\rho_1} + \frac{A_1}{A_2}\right]\frac{1}{c_1^2}\frac{\partial^2 \sigma}{\partial t^2}\bigg|_{0^-,n}$$
$$= \sigma_{+1,n} - \frac{A_1}{A_2}\sigma_{0^-,n} - \frac{c_2\rho_2}{c_1\rho_1}[\sigma_{0^-,n} - \sigma_{-1,n}]. \tag{37}$$

Using (30) and central differences for the second derivative, (37) is rewritten as follows:

$$\sigma_{0^-,n+1} = \frac{2}{1 + \dfrac{A_1\rho_1c_1}{A_2\rho_2c_2}}\sigma_{-1,n} + \frac{2}{\dfrac{A_1}{A_2}\left(1 + \dfrac{A_2\rho_2c_2}{A_1\rho_1c_1}\right)}\sigma_{+1,n} - \sigma_{0^-,n-1} \tag{38}$$

where $n \geqslant 1$. This is the desired difference scheme for the interface boundary. Equation (38) is reduceable to (15) for $m = 0$ when the subscripts are equal, that is, when the discontinuity vanishes.

The difference schemes for the initial time steps, in a manner similar to that demonstrated above for the interior-point case, can be shown as

$$\sigma_{0^-,0} = f(0^-) \tag{39}$$

and

$$\sigma_{0^-,1} = \frac{1}{1 + \dfrac{A_1\rho_1c_1}{A_2\rho_2c_2}}\,\sigma_{-1,0} + \frac{1}{\dfrac{A_1}{A_2}\left(1 + \dfrac{A_2\rho_2c_2}{A_1\rho_2c_1}\right)}\,\sigma_{+1,0} + \Delta t\, g(0^-). \tag{40}$$

The values on the right side of the interface are given by (27)

$$\sigma_{0^+,n} = \frac{A_1}{A_2}\,\sigma_{0^-,n} \qquad \text{for} \quad n \geqslant 0. \tag{41}$$

The complete difference method thus consists of (15), (16), and (19) for the interior points and (38), (39), (40), and (41) for the interface boundaries.

Illustrative Examples

In this section two illustrative examples are solved by the difference method and the results are compared with analytical and available experimental results; good agreements are shown in both cases.

Stepped Bar

For the sake of visualization, an example involving a bar with a single discontinuity in geometry and material was chosen.

The bar is illustrated in Fig. 4. The properties of both sections are related as follows:

$$\frac{A_1}{A_2} = \frac{1}{2}, \qquad \frac{E_1}{E_2} = \frac{1}{2}, \qquad \frac{\rho_1}{\rho_2} = \frac{9}{8}. \tag{42}$$

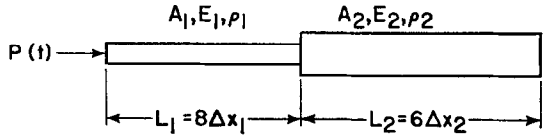

FIG. 4. Stepped bar.

Therefore,

$$\frac{\Delta x_1}{\Delta x_2} = \frac{c_1}{c_2} = \frac{2}{3}. \tag{43}$$

Moreover, the sectional lengths were chosen so that

$$\frac{L_1}{L_2} = \frac{8\Delta x_1}{6\Delta x_2} = \frac{8}{9}. \tag{44}$$

These relationships result in a randomly related transit-time interval:

$$\frac{t_1}{t_2} = \frac{L_1/c_1}{L_2/c_2} = \frac{4}{3}. \tag{45}$$

The initial values were chosen as follows:

$$f(x) = 0 \qquad \text{for} \quad 0 < x < L \tag{46}$$

$$g(x) = 0 \qquad \text{for} \quad 0 < x < L. \tag{47}$$

The end conditions were prescribed:

$$P_1(t) = \begin{cases} 1000 & \text{for} \quad 0 < t < 8\Delta t \\ 0 & \text{for} \quad t \geqslant 8\Delta t \end{cases} \tag{48}$$

$$P_2(t) = 0 \qquad \text{for} \quad t > 0. \tag{49}$$

The uniform initial values and the rectangular input pulse were chosen for ease in verifying results rather than to simplify the problem.

The difference solution was carried out as outlined previously; the results are shown in Fig. 5, where values at the interface, $m = 8$, are shown for the left side only. Since the transit-time intervals were not simply related, interaction of the wave fronts becomes more complicated at the later time steps.

These results can be compared with results obtained by the ray-tracing method, which is easily applied to this simple problem. The familiar coefficients of reflection and transmission are as follows:

$$\frac{\sigma_R}{\sigma_I} = \frac{1 - A_1\rho_1c_1/A_2\rho_2c_2}{1 + \dfrac{A_1\rho_1c_1}{A_2\rho_2c_2}}, \qquad \frac{\sigma_T}{\sigma_I} = \frac{2}{\dfrac{A_2}{A_1}\left(1 + \dfrac{A_1\rho_1c_1}{A_2\rho_2c_2}\right)}. \tag{50}$$

Thus, for right-bound waves

$$\frac{\sigma_R}{\sigma_I} = 0.455, \qquad \frac{\sigma_T}{\sigma_I} = 0.727 \tag{51}$$

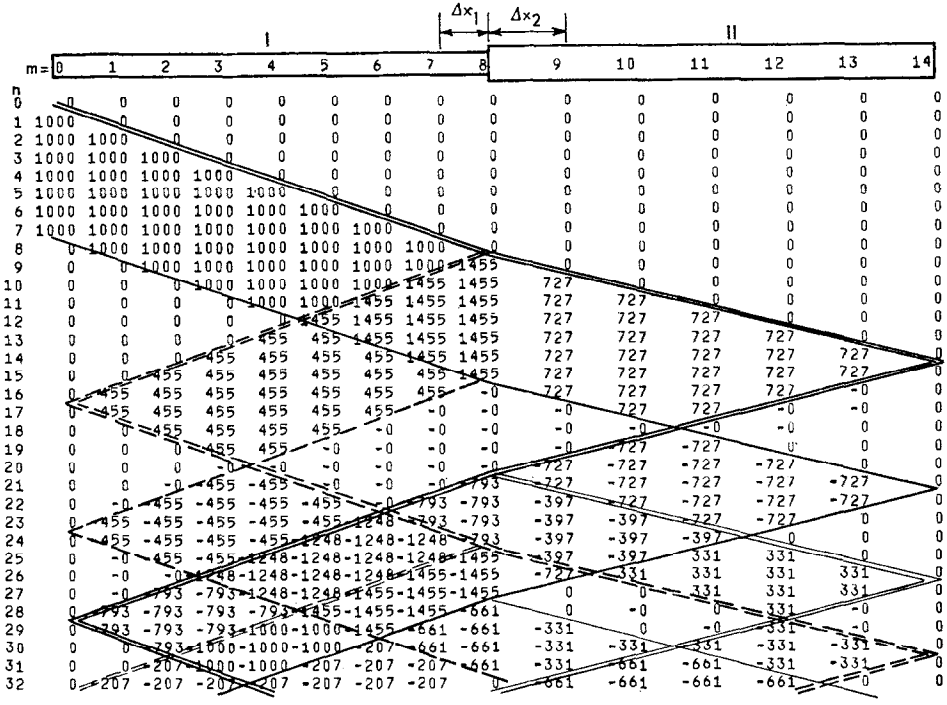

FIG. 5. Stress propagation in a stepped bar.

and for left-bound waves

$$\frac{\sigma_R}{\sigma_I} = -0.455, \qquad \frac{\sigma_T}{\sigma_I} = 1.091. \tag{52}$$

The results obtained by the ray-tracing method are identical to those obtained by the difference method:

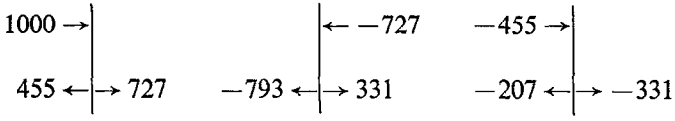

The well-known results of reflection of stress waves at a free end are also evident in Fig. 5.

Necked Rod

For the second example, a case with two geometrical discontinuities was chosen. Experimental data were available for a necked rod studied by Beddoe [4], who

used strain gages to record tensile impact effects. The rod, with four gage locations, is illustrated in Fig. 6. The instrumentation was capable of simultaneously recording two gages only. The experimental data (Figs. 4 to 6 in [4]) chosen for the present study consist of strain records of Gage A together with one of the other gages B, C, and D.

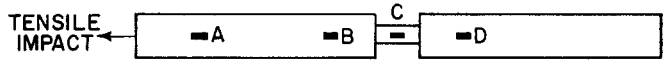

FIG 6. Necked rod.

In the difference solution to this problem, since $\rho_1 = \rho_2$ and $c_1 = c_2$, (38) became

$$\sigma_{0^-,n+1} = \frac{2}{1 + A_1/A_2}(\sigma_{-1,n} + \sigma_{+1,n}) - \sigma_{0^-,n-1}. \tag{53}$$

Proper area ratios were used for the interfaces—in this case one was the reciprocal of the other.

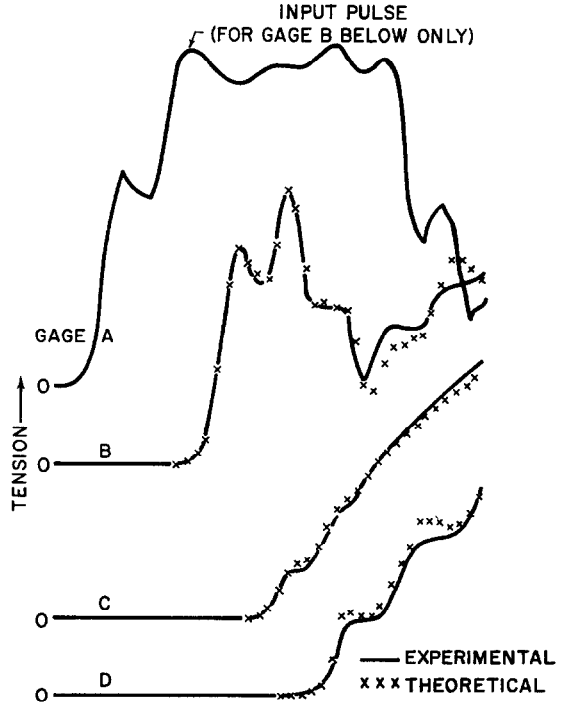

FIG 7. Comparison of results for necked rod.

Since the actual input pulse was unknown, the Gage A location was regarded as the end of the rod, and the Gage A readings were used as input pulse. From Gage A to the free end, the rod was divided into forty-two increments; and the strain histories at all grid points, including the gage locations, were computed. Using the experimentally determined input pulses (Gage A), the corresponding responses at Gages B, C, and D were computed. Good agreement between the experimental and theoretical results is readily shown in Fig. 7.

Discussion

The explicit difference schemes require only two previous time lines to generate a new time line. To calculate an unknown value on a new time line, only three previous known values, lying on and within the characteristic lines, are required. Thus the marching method is simple enough to be amenable to hand computations. With a computer, thousands of spatial meshes and hundreds of discontinuities can be readily handled.

The method, as presented, is restricted by the requirement that segments of the bar on two sides of an interface satisfy

$$N \equiv \frac{L_i c_{i+1}}{c_i L_{i+1}} = \frac{L_i \, \Delta x_{i+1}}{\Delta x_i \, L_{i+1}} = \frac{M_i}{M_{i+1}}, \tag{54}$$

where M is an integer representing the number of meshes in the bar segment. It is therefore implied that N is a rational number. To handle a more general case when N is an irrational number, there are two alternative approaches: (a) Choosing M_i and M_{i+1} large enough so that N is approximated to a desired accuracy. This is feasible because the method allows a large number of spatial meshes. (b) Choosing the mesh sizes such that $c \, \Delta t/\Delta x < 1$. After the required modifications in Equations (15) through (40), the difference solution would still satisfy the stability condition (13) while keeping the spatial meshes to a reasonable number.

The difference method which has been used in the investigation of viscoelastic waves in a split Hopkinson pressure bar [9], is readily applicable to bars of greater complexity. Because of its ability to handle a large number of discontinuities, the difference method is highly suitable also for solving, by means of realistic incremental approximation, problems involving continuous change in physical properties such as the bars with a temperature gradient [10]. On the other hand, the method is as good as the assumption that the elementary theory of the one-dimensional stress waves prevails. In the case of uniform bars the elementary theory is valid for waves with long wave lengths [2, 11]. In the case of bars with

discontinuities the range of validity of the theory is expected to be more restricted as indicated by the experimental evidences [2–4].

REFERENCES

1. J. PRESCOTT, "Applied Elasticity," pp. 257–261. Dover, New York, 1961.
2. H. C. FISCHER, *Appl. Sci. Res.* **A-8** (1957), 105–139, 278–308.
3. E. A. RIPPERGER AND H. N. ABRAMSON, "Reflection and Transmission of Elastic Pulses in a Bar at a Discontinuity in Cross Section," pp. 135–145, Proc. Midwestern Conf. Solid Mech., 3rd, 1957.
4. B. BEDDOE, *J. Sound Vib.* **2** (1965), 150–166.
5. V. H. KENNER AND W. GOLDSMITH, *J. Acoust. Soc. Amer.* **45**, 115–118 (1969).
6. K. J. DEJUHASZ, *J. Franklin Inst.* **247** (1949), 15–45.
7. R. P. REED, Stress Pulse-Trains from Multiple Reflection at a Zone of Many Discontinuities," Research Report SC–4462 (RR). Sandia Laboratories, Albuquerque, New Mexico, 1962.
8. R. D. RICHTMYER AND K. W. MORTON, "Difference Methods for Initial-Value Problems," pp. 9–16, 260–263, Wiley (Interscience), New York, 1967.
9. S. S. CHIU AND V. H. NEUBERT, *J. Mech. Phys. Solids* **15** (1967), 177–193.
10. J. L. CHIDDISTER AND L. E. MALVERN, *Expt. Mech.* **3** (1963), 81–90.
11. H. KOLSKY, "Stress Waves in Solids," pp. 73–74, Dover, New York, 1963.